SARCOIDOSIS VASCULITIS AND DIFFUSE LUNG DISEASES 2015; 32; 342-352

Characterization of F-18 Fluorodeoxyglucose PET/CT in granulomatosis with polyangiitis

Darlene R. Nelson[1], Geoffrey B. Johnson[2], Rodrigo Cartin-Ceba[1], Ulrich Specks[1]
[1] Division of Pulmonary and Critical Care Medicine and [2] Department of Radiology and Immunology, Mayo Clinic, Rochester, MN

Abstract. *Objective:* Granulomatosis with polyangiitis (GPA) is a rare autoimmune disease characterized by necrotizing granulomatous inflammation and small vessel vasculitis that primarily involves the upper airways, lungs, and kidneys. F-18-fluorodeoxyglucose (FDG) positron emission tomography (PET) is an imaging technique that is increasingly used in the evaluation of patients with other types of vasculitis (giant-cell arteritis). We explored the potential utility of FDG-PET/CT in the management of GPA. *Methods:* We identified 12 patients with GPA who underwent a total of 26 FDG-PET/CT scans from January 2005 to March 2013. The presenting clinicoradiologic features and FDG-PET/CT scans were analyzed. *Results:* In all patients the FDG-PET/CT scans were performed to evaluate known or suspected malignancies. Differentiation between inflammatory and malignant lesions could not be achieved based on FDG uptake intensity (maximal SUV). GPA lesions of the respiratory tract and lung were more clearly detected by FDG-PET/CT than by CT scan alone. In 3 of the 12 patients occult areas of vascular inflammation were identified that were not previously appreciated on usual organ screening in GPA. In 8 patients the FDG-PET/CT facilitated diagnosis by identifying the best biopsy site. Two patients had follow-up FDG-PET/CT scans which demonstrated decreased FDG uptake after treatment for GPA. *Conclusions:* FDG-PET/CT cannot differentiate between malignant and inflammatory lesions in GPA. However, occult sites of disease activity may be identified and provide a better assessment of the extent of disease activity and a more accurate assessment of treatment response. *(Sarcoidosis Vasc Diffuse Lung Dis 2015; 32: 342-352)*

Key words: ANCA-associated vasculitis, FDG-PET/CT, Granulomatosis with polyangiitis (Wegener's)

Introduction

Granulomatosis with polyangiitis (GPA, formerly known as Wegener's granulomatosis) is a rare autoimmune disease that is characterized by necrotizing granulomatous inflammation and small vessel vasculitis. It primarily involves the upper airways, lungs, and the kidneys (1). Early and accurate diagnosis and assessment of the extent of the disease is important for treatment decisions. In clinical practice, diagnosing GPA early and evaluating the extent and location of the disease accurately can be a challenge. F-18-fluorodeoxyglucose (FDG) positron emission tomography (PET) has been used for several years in oncology to image metabolically active tissue. FDG is a glucose analog labeled with a fluorine-18 nuclide, which is a positron emitter used in

Received: 22 September 2014
Accepted after revision: 24 March 2015
Correspondence: Ulrich Specks, MD,
Division of Pulmonary and Critical Care Medicine,
Gonda 18, Mayo Clinic,
200 1st St. SW, Rochester, MN 55905
Tel. 507-284-3811
Fax 507 266-4372
E-mail: specks.ulrich@mayo.edu

clinical imaging. It is taken up into cells via the same mechanism as glucose though the Glut-1 transporter then becomes phosphorylated and trapped in the cell. Because FDG lacks a 2' hydroxyl group it cannot be dephosphorylated or broken down in the Krebs cycle. Therefore the distribution of FDG is a good reflection of glucose uptake which is increased in malignant cells and immune cells involved in inflammation (2).

Recently, FDG-PET/CT is gaining wider acceptance as a useful tool in the diagnosis and management of inflammatory processes. FDG-PET/CT scans commonly demonstrated FDG activity in inflammatory conditions including infections and interstitial lung diseases, such as sarcoidosis, idiopathic pulmonary fibrosis and rheumatoid arthritis-associated lung disease. In addition, several reports have proposed clinical utility in large-vessel vasculitis such as giant cell arteritis and Takayasu's arteritis (3-7). FDG-PET/CT has the potential to accelerate definitive treatment of these vasculitides by non-invasively diagnosing and localizing disease activity earlier than can be achieved with traditional anatomical imaging modalities. The role of FDG-PET/CT in the diagnosis of small vessel vasculitis is less well defined. The goal of this study was to identify FDG-PET/CT scan abnormalities associated with GPA in adults and to describe clinical, pathologic and radiologic associations.

Patients and methods

Patient selection

A computer-aided search was conducted to identify all adults (≥18 years of age) who were seen at the Mayo Clinic (Rochester, MN) from January 1, 2005 to March 31, 2013 who had received a diagnosis of GPA and had undergone FDG PET/CT scanning. Patients were consecutively included and had received a diagnosis of GPA based on clinical, serologic and pathologic findings and fulfilled the 1990 American College of Rheumatology criteria and the Chapel Hill consensus definition (8). The Mayo Foundation Institutional Review Board approved this study. Patients who did not authorize the use of their medical records for research were excluded from this study.

Clinical laboratory and radiologic findings

Data extracted from the medical records included age, gender, primary symptoms, method of diagnosis, delay from diagnosis of vasculitis, ANCA testing, acute phase reactants, organ involvement, treatment, findings on lung and sinonasal CT scans, FDG PET/CT scans, and the clinical course of each identified patient. For disease activity, the Birmingham Vasculitis Activity Score (BVAS/WG) was assessed (9).

FDG-PET/CT scan imaging

All PET scans were systematically reviewed, and the maximum standardized uptake value (max SUV) was determined by a nuclear radiologist (GBJ). All but 2 FDG PET/CT studies were performed at our institution. FDG PET/CT was performed according to our institutional standard clinical protocol on Discover LS (2 more remote studies) and Discovery RX or 690 (all subsequent scans) scanners (GE Medical Systems, Waukesha, WI). Weight, height, and age at time of scan were recorded for all patients. All patients had a blood glucose level of less than 200 mg/dL at the time of injection. 18F-FDG was synthesized using an onsite cyclotron and a commercial synthesis module (TracerLab, GE Medical Systems, Waukesha WI). All patients received an intravenous injection of 12–17 MBq 18F-FDG with an uptake time of 60-70 minutes post injection. Patients were imaged with arms up, from orbits to mid-thigh. Reconstruction of the PET images on the Discovery RX, and 690 scanners was performed with a 3-D ordered-subset expectation maximization algorithm, and 2-D algorithms were used for the Discovery LS scanners. Low dose helical CT images were obtained for attenuation correction and images were fused by bed position for anatomic localization (detector row configuration 16 x 0.625mm, pitch 1.75, gantry rotation time 0.5 s, slice thickness 3.75mm, 140 kVP and mAs range of 60-120 using automatic current-modulation). 2 patients had FDG PET/CT performed on a 2-D scanner at an outside institution.

A positive PET was defined as the presence of an uptake higher than expected for a given tissue (such as higher than blood pool in a lymph node) and not explained by physiological processes (10). The following

sites were systematically analyzed: lung, sinonasal mucosa, bone and cartilage, lymph nodes, submandibular and parotid glands, bone marrow, spleen, kidney, thyroid, heart, pineal gland, large vessels and perivascular areas. Pathologic FDG uptake was correlated to CT findings and the maximum SUV was determined for any site of abnormal FDG uptake.

Statistical analysis

All continuous data are summarized as medians with inter quartiles 25-75 [IQ 25-75] and frequencies with percentages for qualitative variables. Difference in medians between groups was tested with the Wilcoxon sum rank test. P-values of <0.05 were considered statistically significant. JMP statistical software (version 9.0, SAS, Cary, NC) was used for all analyses.

Results

Demographic and clinical features

Twelve patients with GPA underwent a total of 26 FDG-PET/CT scans during the study period; pertinent demographic and clinical data are included in Table 1. The mean age of the GPA cohort was 69 years of age [63.5-74.5]; nine patients (69.2%) were women. Eight of the scans were done at the time of GPA diagnosis and 19 during follow up. Seven of the patients had abnormal PR3- or MPO-ANCA

Patient 1:

Table 1. Characteristics of patients with ANCA-associated vasculitis at time of initial PET/CT scan

Characteristics Age (years)	All patients (n=12) 69 (63.5-74.5)	GPA alone (n=8) 69 (66.577.5)	GPA + malignancy (n=4) 63.5 (44.75-68)
Gender (male)	3	1	2
Involved organs (n)			
Constitutional signs	6	3	3
Lung	10	6	4
Kidney	5	3	2
ENT	7	4	3
Eye	3	3	0
Gastrointestinal tract	1	0	1
Cardiovascular	2	2	0
Skin/joint	6	4	2
Nervous system	2	2	0
Laboratory data (normal values)			
WBC (*3.5-10.5x10(9)/L)*	8,000 (5,525-9,550)	7,300 (4,700-12,850)	8,500 (8,300-9,100)
Creatinine (*M: 0.8-1.3 mg/dL; F: 0.6-1.1 mg/dL*)	0.8 (0.7-0.97)	0.8 (0.7-0.95)	0.9 (0.7-1.3)
ESR (*M: 0-22 mm/hr; F: 0-29 mm/hr)*	34 (16-59)	29 (11.5-89.75)	34 (29-36)
C-reactive protein *(< or =8.0 mg/L*)	10.2 (4.75-33.82)	10.2 (4.53-91.02)	22.25 (4.4-40.1)
ANCA positive	10	6	4
PR3 *(<0.4U)*	3	3	0
MPO *(<0.4 U)*	4	3	1
BVAS-WG	2 (0.5-5)	2 (1.5-4)	2.5 (0-6.5)
BVAS-WG >1	10	8	2
SUVmax (median)	7.6 (3.12-14)	7.6 (4.65-15.88)	6.45 (2.5-13.18)
Delay PET from diagnosis (months)	0.5 (-0.5-25)	19 (4.37-26.5)	0 (-1.5-105)

Abbreviations: BVAS-WG (Birmingham vasculitis activity score for Wegener's granulomatosis), ENT (Ear nose and throat), M (Male), F (Female)

Table 2. Imaging Characteristics of FDG PET/CT and correlation with pathology on initial scans in GPA alone patients

Pt #	Indication	FDG uptake location	SUVmax	Shape on CT findings	Pathology
1	Pulmonary nodules	left upper lobe, right lower lobe	4.1	Multiple pulmonary nodules	No biopsy
		Hilar lymph nodes	4.8	Mildly enlarged hilar lymph nodes	No biopsy
2	Mesenteric lymphadenopathy	None	-	Slightly enlarged mesenteric lymph nodes	No biopsy
3	Pulmonary nodule	Right upper and lower lung, left maxillary sinus	8.6	Nodular infiltrate right upper lobe and cavitary lesion right lower lobe,	No biopsy
		Left maxillary sinus	3.7	Mild mucosal thickening left maxillary sinus	No biopsy
		Left subglottic trachea	2.7	Tracheal irregularity/thickening	No biopsy
4	Pulmonary mass	Right lower lung	6.6	Large oval solid mass	Necrotizing granulomatous inflammation
		Subcarinal lymph node	3.9	Mildly enlarged subcarinal lymph node	No biopsy
5	Pulmonary nodules	Bilateral lungs	6.3	Multiple nodular opacities	Necrotizing granulomatous inflammation
		Lymph nodes	3.2	Mildly enlarged left internal mammary and right paraspinal	No biopsy
		Skin and subcutaneous tissue	2.5	Subtle nonspecific skin thickening and fat stranding	No biopsy
		Right femoral artery	5.5	Normal appearing vessel	No biopsy
7	Orbital mass	Right orbit and optic nerve	10.0	Soft tissue mass involving the right orbit and right lacrimal gland	Necrotizing granulomatous inflammation
		Right lacrimal gland	6.0	Normal appearing gland	No biopsy
		Right maxillary sinus		Mild mucosal thickening	No biopsy
10	Pulmonary nodules	Bilateral lungs	13.4	Scattered bilateral pulmonary nodules	Necrotizing granulomatous inflammation
		Nasal mucosa and sinuses	16.8	Fluid in right sphenoid sinus, nasal mucosa normal on CT	No biopsy
12	Pulmonary nodules	Bilateral lungs	16.7	Lobulated consolidative mass, rounded nodule, right pleural effusion, atelectasis	Fibrinous pleuritis
		Right main bronchus	3.9	Circumferential thickening of the short segment of the right main stem bronchus	No biopsy
		Nasal passages	12.5	Mucosal thickening and fluid throughout sinuses	No biopsy

levels. No significant correlation was found between max SUVs and the laboratory data (WBC, Hgb, CRP, ESR, creatinine, PR3-ANCA titer and MPO-ANCA titer, p=NS). Four patients were on immunosuppression at the time of initial FDG-PET/CT (nos. 1, 2,6 and 11).

Indications for all of the FDG-PET/CT scans were for known or suspected malignancy. Four of the 12 patients were diagnosed with concurrent malignancy and GPA after biopsies were performed. Two of these patients were also found to be having an active GPA flare at the time of their cancer diag-

Table 3. Imaging Characteristics of FDG PET/CT and correlation with pathology on initial scans in GPA + malignancy patients

Pt #	Indication	FDG uptake location	SUV max	Shape on CT findings	Pathology (Tumor staging)
6	Pulmonary mass	Left lung and pleural fluid	14.2	Lobulated and spiculated mass	Adenocarcinoma (T3, N2, M1a)
		Mediastinal and hilar lymph nodes	10.9	Mildly enlarged lymph nodes	No biopsy
8	Nasopharyngeal mass	Left lung	2.4	Cavitated solid nodule	No biopsy
		Nasopharynx	9.3	Masslike invasive process centered in the left nasopharynx	Diffuse large B cell lymphoma and necrotizing granulomatous inflammation (Stage IVB with concomitant GPA)
		Aortic arch	5.9	Soft tissue density between ascending aorta and right ventricular outflow tract	No biopsy
9	Lung mass, previous history of melanoma (T1, NO, MO)	Bilateral lungs	10.1	Left upper lung subpleural consolidation, right lower lobe nodule	Necrotizing granulomatous inflammation
		Aortic arch	4.9	Non-circumferential thickening of the anterior aortic arch	No biopsy
		Mediastinal and hilar lymph nodes	3.3	Mildly enlarged mediastinal lymph nodes	No biopsy
		Left orbit	4.6	No mass lesion	No biopsy
		Nasal passages	3.8	No mucosal thickening	No biopsy
11	Staging for lung cancer	Bilateral lungs	2.8	Consolidative infiltrates in both lungs, fibrotic lung disease, atelectasis	Adenocarcinoma (T2, N1, M0)

nosis. Of the patients without malignancy 7 of the 8 patients (87.5%) had positive findings on FDG-PET/CT scan. The characteristics of the patients with malignancy have been separated out (Table 1).

Results of the FDG-PET/CT scans in the 8 patients with GPA alone led to biopsy and subsequent new diagnosis of GPA in 5 patients and diagnosis of a flare of GPA in 2 patients. One patient with a negative PET scan was referred for symptoms that could not be reconciled with the preexisting diagnosis of GPA (mesenteric lymphadenopathy). Nine of the twelve patients in our case series that underwent a biopsy had the location guided by FDG-PET/CT. For example, in case no. 9, the patient had previous diagnosis of melanoma (not currently on treatment), FDG uptake was noted in both a cervical lymph node as well as multiple pulmonary nodules. The pulmonary nodules were more suggestive of a GPA flare than metastatic disease. Consequently biopsies were performed of both a cervical lymph node and a pulmonary nodule. The pathology showed relapsed melanoma from the cervical node and necrotizing granulomas from the pulmonary nodule consistent with a diagnosis of GPA.

Radiologic features

There was no significant difference between inflammatory and malignant images based on FDG-PET/CT imaging (Tables 2 and 3). The median max SUV for lung lesions that were malignant was 6.45 [2.5-13.2] versus 7.6 [4.6-15.9] for GPA; p = NS. In patients with GPA alone, the most common areas with FDG uptake were the lungs (75%) and si-

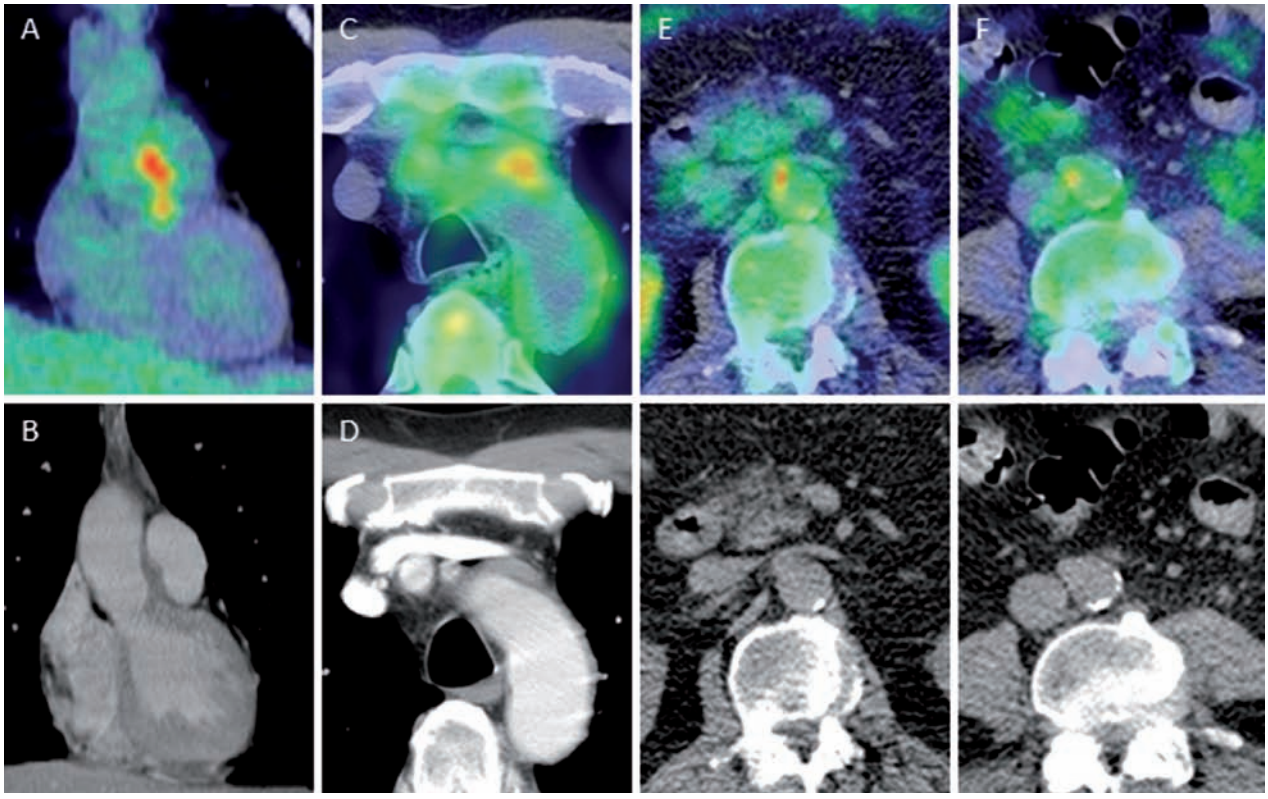

Fig. 1. Arterial wall involvement with GPA. Patient no. 8 shows intensely FDG avid fusiform non-calcified non-circumferential thickening of the ascending aorta wall just distal to the aortic valve, between the aorta and main pulmonary artery seen on coronal fused PET/CT (A) and diagnostic IV contrast enhanced coronal CT performed 1 day earlier (B). This thickening and activity slowly resolved on follow-up PET/CT scans with therapy for GPA. This patient also had lymphoma, and this tissue was never directly biopsied, so the diagnosis of GPA in this location is not certain. Rarely lymphoma can involve vessel walls in a similar manner. Patient no. 9, at the time of diagnosis of GPA, showed intensely FDG avid fusiform non-calcified non-circumferential thickening of the anterior aortic arch extending into the wall of the left subclavian artery as seen on axial PET/CT (C) and IV enhanced axial diagnostic CT (D) that resolved on follow up imaging with therapy for GPA. Three years later, at the time of a flair in GPA activity seen elsewhere in the lungs on FDG PET/CT (9/27/10 on figure 5), there was new focal moderately FDG avid fusiform non-calcified non-circumferential thickening in the right wall of the aorta at the level of the right renal artery and at the aortic bifurcation seen on axial PET/CT (E & F). This patient had a history of melanoma, but these lesions resolved with therapy for GPA, which would not be expected for melanoma. Although one might question whether the lesions represented in E & F are focal vulnerable plaque from atherosclerotic disease, the lesions bulged out the contour of the aorta and later shrank with GPA therapy, which would be uncharacteristic of atherosclerosis

nuses (50%). GPA lesions of the respiratory tract and lung were more clearly detected on F18 FDG-PET/CT scan than CT alone. This is illustrated by case no. 9, in which mild increased FDG activity was noted in the nasal passages (SUV max 3.8), with no clear nasal mucosal thickening on the CT.

In addition to the usual sinonasal and lung involvement in patients with GPA, FDG-PET/CT demonstrated pathologic uptake in several areas. Mediastinal and hilar lymph node uptake was observed in 3/8 (37.5%) patients with GPA alone. All were associated with lung involvement. Diffuse bone marrow and spleen uptake were observed in 1/8 cases with GPA alone and 1/4 cases with concurrent malignancy. No pathologic kidney uptake was appreciated in our patient series. Finally, FDG uptake in major vessels that was not previously appreciated by standard diagnostic modalities was noted in 3 patients (Figure 1). Each of these lesions (cases #5, 8 and 9) had areas of focal, fusiform shaped, asymmetric vessel wall inflammation with no calcification and intense FDG activity. This is differentiated from atherosclerosis

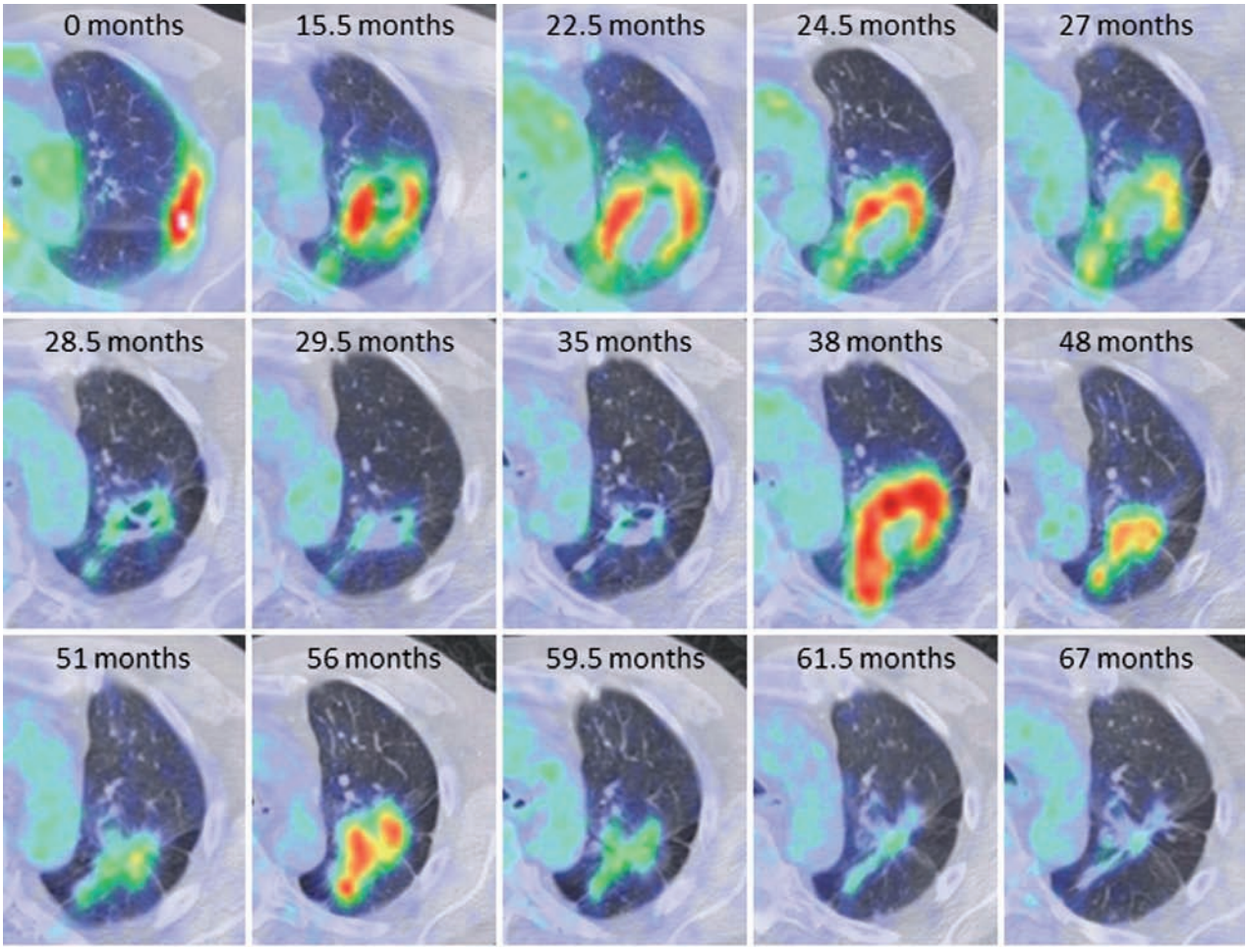

Fig. 2. Following GPA in FDG PET/CT in a cancer patient. GPA in the left upper lobe that was twice biopsy proven shows the how FDG activity seen on PET and the changes on CT complement each other in assessing the response to therapy and subsequent flairs of GPA over time. All images are axial PET/CT. This patient (no. 9) had recurrent metastatic melanoma in the neck, and the PET/CT scans were performed primarily to follow the melanoma. At 28.5 months since his initial PET/CT, right neck lymph nodes were increasing in FDG activity, as opposed to the decreasing activity in the known GPA in the lung, and these nodes proved to be recurrent melanoma. At 48 months, a focus of FDG activity was identified in the colon that was increasing in activity, again as opposed to the decreasing activity in the known GPA in the lung at that time, and the colon lesion proved to be an incidental primary colon adenocarcinoma. Therefore multiple FDG PET/CT scans over time can help to follow cancer and GPA, and at times can help to differentiate between the two. However, as exemplified in figure 1, in a given lung lesion on a single scan, neither FDG PET/CT nor diagnostic CT can confidently differentiate between active GPA and cancer

which generally is more diffuse with scattered intraluminal calcifications and mild patchy circumferential thickening and milder or background FDG activity.

Treatment response evaluation

Of the total, two patients (Nos. 8 and 9) had follow-up FDG-PET/CT scans as follow-up for a concurrent history of malignancy. Case no. 8 was given a simultaneous diagnosis of large B cell lymphoma (Stage IVB) and GPA in the nasopharynx and lung. The patient was noted to have persistent activity on FDG-PET/CT scan despite multiple chemotherapeutic regimens. She ultimately underwent a nasal biopsy which demonstrated persistent inflammation consistent with GPA. The lesion subsequently resolved (FDG avidity decreased) after treatment with high dose prednisone. Case no. 9 had

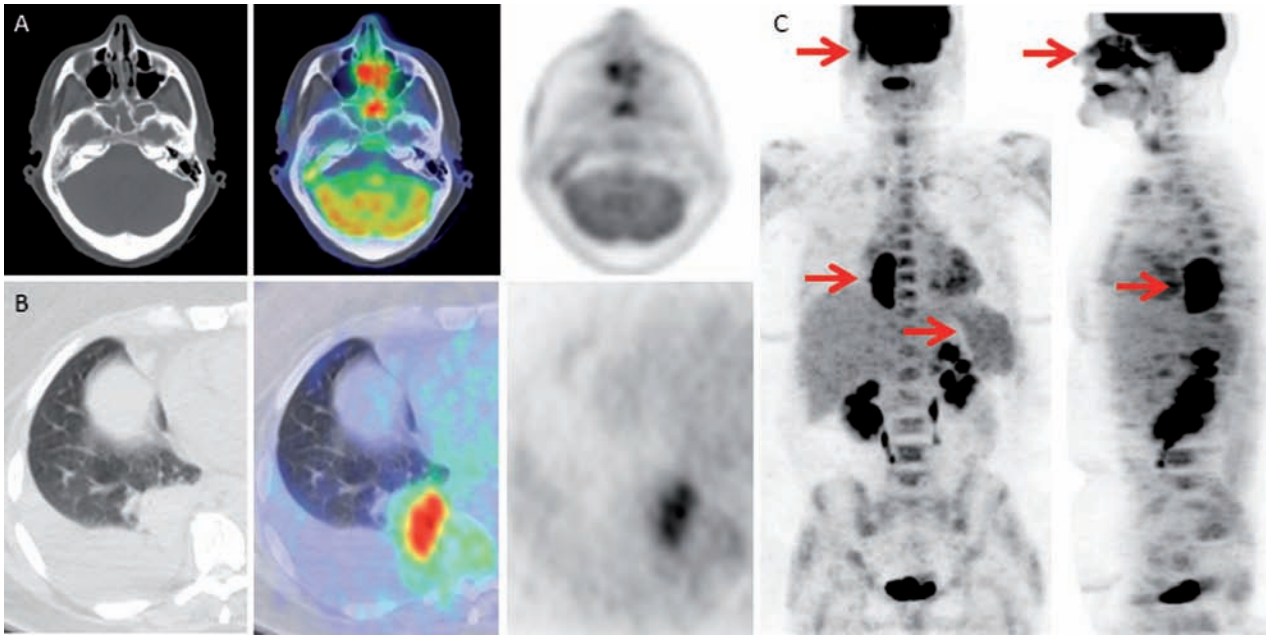

Fig. 3. Multifocal Disease pattern on PET/CT suggests GPA. Patient no. 12 has a multifocal disease seen on PET/CT fits a pattern highly suggestive of GPA, including FDG avid lung and sinus disease. Intense FDG activity in the nasal mucosa and sphenoid sinuses with no clear underlying mass seen on axial PET/CT (A) and sagittal MIP PET image (C, arrow). Secondary obstructive non-FDG avid fluid in the sphenoid sinuses. The FDG activity in the nasal cavity and sinuses far exceeds that seen with more common etiologies of inflamed nasal and sinus mucosa, indicating this is not simple sinusitis. In addition, the right eustachian tube also had increased FDG activity likely due to GPA seen on frontal view of the MIP PET image (C, arrow) with non-FDG avid fluid in the right mastoid air cells (not shown). A right ear cholesteatoma was considered a possible diagnosis based on CT prior to the PET/CT. Intensely FDG avid solid sub-pleural lung mass with air bronchograms is seen on axial PET/CT (B) and MIP PET images (C, arrows) proved to be GPA. Adjacent non-FDG avid pleural effusion. Diffuse bone marrow and splenic FDG activity, which is seen in several cases of GPA at the time of initial diagnosis is seen on MIP PET images (C, arrow on spleen). The lung mass considered by itself on CT and PET/CT could easily be confused with malignancy. However, the pattern of activity in the lung and nasal passages should put GPA at the top of the differential. This patient had normal renal function, but the kidneys look similar on FDG PET/CT to those with GPA involvement seen in other patients on PET/CT, likely due to high urine background activity

a previous diagnosis of malignant melanoma (T1, N0, M0) and GPA. FDG-PET/CT scans were performed to evaluate for recurrence of his melanoma (Figure 2). His initial scan at our institution demonstrated increased FDG avidity in pulmonary nodular lesions consistent with a flare of his known GPA. After re-treatment with rituximab and corticosteroids the FDG uptake decreased in response to treatment. Subsequent FDG-PET/CT scans have consistently shown increased FDG avidity when the patient is having a flare of GPA that responds to treatment with further immunosuppression.

Discussion

In this case series we retrospectively explored the potential utility of FDG-PET/CT in the diagnosis and follow-up of GPA. Although FDG-PET/CT scanning is currently not routinely performed in the evaluation of patients with GPA, it may be obtained in certain clinical contexts. Lung involvement in GPA may manifest as lung nodules, which are often cavitary, whereas mediastinal lymphadenopathy and pleural effusions are rare (11) Depending on the clinical context, the presence of any of these radiographic findings may raise concern for malignancy and prompt further diagnostic testing, including FDG-PET/CT scan.

The diagnosis of GPA is occasionally delayed as patients often present with nonspecific symptoms such as fever, malaise, weight loss and myalgia. Several anatomical imaging modalities are used to diagnose vasculitis including MRI and CT. However these modalities can only demonstrate anatomical changes

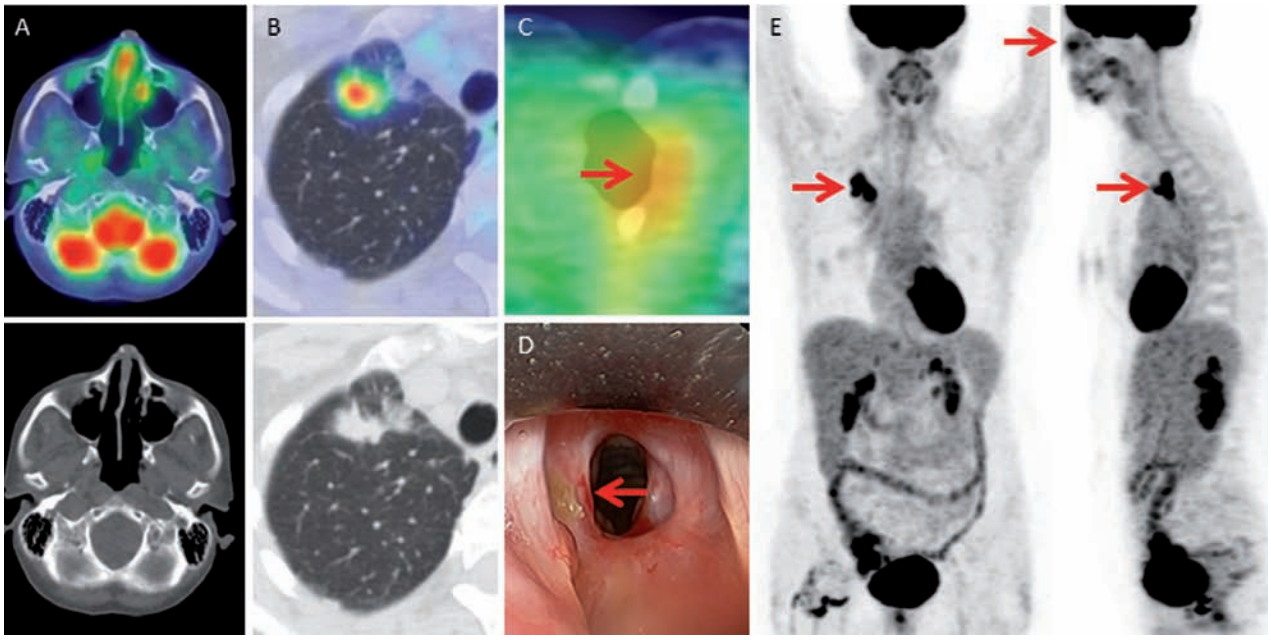

Fig. 4. PET/CT in Recurrent GPA. Multifocal disease seen on PET/CT fits a pattern highly suggestive of GPA in this patient (no. 3) with recurrent GPA disease, including FDG avid lung, sinus and tracheal disease. Moderate FDG activity in the nasal mucosa with no clear underlying mass seen on axial PET/CT (A) and sagittal MIP PET image (E, arrow). Multiple intensely FDG avid solid and part-solid lung nodules seen on axial PET/CT (B) and MIP PET images (D, arrows). Mild activity in the left subglottic trachea seen on axial PET/CT (C, arrow) matches a focus of biopsy proven recurrent GPA in the airway seen on bronchoscopy (D, arrow, patient airway is viewed from above/cranial and therefore flipped in relation to the orientation of PET/CT). This patient had prior GPA in the trachea and previous interventions to diagnose and treat this process. Activity in the right hip seen on MIP PET images (D) is related to a healing THA. This patient with recurrent GPA did not show the diffuse splenic and bone marrow activity sometimes seen in the cases of newly diagnosed GPA

that develop once the inflammatory process is well established and they are unreliable for the diagnosis of early inflammatory changes that are potentially reversible. Consequently, there has been an increasing role for FDG PET/CT in the diagnosis and management of large-vessel vasculitides (2). Its role in small vessel vasculitis (GPA, microscopic polyangiitis (MPA), eosinophilic granulomatosis with polyangiitis (EGPA)) is less well defined. Recently two cases series and several case reports have been published on FDG PET/CT findings in patients with GPA (3, 12-20). All of these reports demonstrate that disease activity is accurately identified with FDG PET/CT. As a result, several have suggested that FDG PET/CT may be useful for early diagnosis as well as assessment of treatment efficacy in patients with GPA. One case reported the FDG PET/CT findings preceded a rise in PR3 (21). Our findings from this case series corroborate this notion (Figures 3 and 4). All of the patients with active GPA had positive findings on FDG PET/CT, and a remarkable decrease in FDG uptake was associated with the improvement of symptoms in two patients who had follow-up PET scans (Figure 2). This indicates that FDG uptake correlates with disease activity in GPA.

Soussan et al. have recently described a series of 16 patients with GPA who underwent a total of 21 FDG PET/CT scans (19). All of the patients with GPA who had active disease had positive scans. The scans accurately identified disease activity in lungs, sinonasal, cardiovascular and renal disease. In addition, SUVmax was associated with several disease activity markers (19). However, these authors did not find any occult areas of disease activity not detected by usual organ screening. Therefore, they concluded that there is no role for FDG PET/CT in the evaluation of GPA. This is in contrast with our observations. We identified three patients with active vascular involvement by FDG PET/CT that was not previously identified during their evaluation

for GPA with standard imaging studies (Figure 1). Large vessel inflammation is rare in AAV, however, two cases of asymptomatic aortitis in GPA were recently reported (17, 22). In our series, two patients had involvement of the aortic arch that was asymptomatic. FDG PET/CT may provide new insights into large vessel involvement as part of the spectrum of GPA.

Even though our results show that FDG uptake correlates with the inflammatory activity of GPA, FDG PET/CT scanning does not allow it's differentiation from malignancy. This is similar to what has been reported in other granulomatous and non-malignant thoracic disorders (23, 24). In other granulomatous conditions (cardiac sarcoid) FDG PET/CT has a role in monitoring disease activity but not in differentiating active granulomatous lesions from malignant lesions (25).

Our study has several limitations. The first is the small sample size (12 patients and 26 scans). The second limitation is the variability of time intervals between diagnosis of GPA, treatment and FDG PET/CT scans between patients. We acknowledge that each of these scans was obtained not as a diagnostic study for GPA but to look for evidence of malignancy. This is also the reason why we were only able to demonstrate remission status with FDG PET/CT in the follow-up of two patients. A third limitation is the patient selection bias. All but two of our patients had predominantly pulmonary manifestations of GPA which may not be representative of the spectrum of GPA patients.

In conclusion, FDG PET/CT cannot be used to differentiate between malignant and active inflammatory lesions in patients with GPA based on SUV max. However, FDG PET/CT may be useful to identify vascular involvement that is not readily identified by other imaging modalities and to assess the extent and specific localization of disease activity. In individual cases FDG PET/CT may, therefore, provide valuable guidance for the management of the disease. It may direct towards the most appropriate biopsy site, it may change the categorization of the patient's disease severity with treatment implications, and it may allow a more accurate assessment of the treatment response. The specific clinical utility of FDG PET/CT in the management of patients with GPA deserves further formal study.

Acknowledgments

Dr. Nelson and Dr. Specks had full access to all of the data in the study and take responsibility for the integrity of the data and the accuracy of the data analysis.

Study concept and design: Cartin-Ceba, Nelson, and Specks

Acquisition of data: Johnson and Nelson

Analysis and interpretation of data: Cartin-Ceba, Johnson, Nelson and Specks

Drafting of the manuscript: Cartin-Ceba, Johnson, Nelson and Specks

Critical revision of the manuscript for important intellectual content: Cartin-Ceba, Johnson, Nelson and Specks

Statistical analysis: Cartin-Ceba and Nelson

Study supervision: Specks

References

1. Jennette JC, Falk RJ, Bacon PA, et al. 2012 revised International Chapel Hill Consensus Conference Nomenclature of Vasculitides. Arthritis Rheum 2013; 65 (1): 1-11.
2. Zerizer I, Tan K, Khan S, et al. Role of FDG-PET and PET/CT in the diagnosis and management of vasculitis. Eur J Radiol 2010; 73 (3): 504-9.
3. Bleeker-Rovers CP, Bredie SJ, van der Meer JW, Corstens FH, Oyen WJ. Fluorine 18 fluorodeoxyglucose positron emission tomography in the diagnosis and follow-up of three patients with vasculitis. Am J Med 2004; 116 (1): 50-3.
4. Brodmann M, Lipp RW, Passath A, Seinost G, Pabst E, Pilger E. The role of 2-18F-fluoro-2-deoxy-D-glucose positron emission tomography in the diagnosis of giant cell arteritis of the temporal arteries. Rheumatology (Oxford) 2004; 43 (2): 241-2.
5. Blockmans D, de Ceuninck L, Vanderschueren S, Knockaert D, Mortelmans L, Bobbaers H. Repetitive 18F-fluorodeoxyglucose positron emission tomography in giant cell arteritis: a prospective study of 35 patients. Arthritis Rheum 2006; 55 (1): 131-7.
6. Besson FL, Parienti JJ, Bienvenu B, et al. Diagnostic performance of (1)(8)F-fluorodeoxyglucose positron emission tomography in giant cell arteritis: a systematic review and meta-analysis. Eur J Nucl Med Mol Imaging 2011; 38 (9): 1764-72.
7. Besson FL, de Boysson H, Parienti JJ, Bouvard G, Bienvenu B, Agostini D. Towards an optimal semiquantitative approach in giant cell arteritis: an (18)F-FDG PET/CT case-control study. Eur J Nucl Med Mol Imaging 2014; 41 (1): 155-66.
8. Leavitt RY, Fauci AS, Bloch DA, et al. The American College of Rheumatology 1990 criteria for the classification of Wegener's granulomatosis. Arthritis Rheum 1990; 33 (8): 1101-7.
9. Stone JH, Hoffman GS, Merkel PA, et al. A disease-specific activity index for Wegener's granulomatosis: modification of the Birmingham Vasculitis Activity Score. International Network for the Study of the Systemic Vasculitides (INSSYS). Arthritis Rheum 2001; 44 (4): 912-20.
10. Peller PJ. PET/CT Interpretation. In: Patrick Peller RS, Ali Guermazi, ed. PET-CT and PET-MRI in Oncology: Springer Berlin Heidelberg; 2012: 31-44.
11. Cordier JF, Valeyre D, Guillevin L, Loire R, Brechot JM. Pulmonary Wegener's granulomatosis. A clinical and imaging study of 77 cases. Chest 1990; 97 (4): 906-12.

12. Watts RA, Al-Taiar A, Scott DG, Macgregor AJ. Prevalence and incidence of Wegener's granulomatosis in the UK general practice research database. Arthritis Rheum 2009; 61 (10): 1412-6.
13. Almuhaideb A, Syed R, Iordanidou L, Saad Z, Bomanji J. Fluorine-18-fluorodeoxyglucose PET/CT rare finding of a unique multiorgan involvement of Wegener's granulomatosis. Br J Radiol 2011; 84 (1006): e202-4.
14. Nishiyama Y, Yamamoto Y, Dobashi H, Kameda T. Clinical value of 18F-fluorodeoxyglucose positron emission tomography in patients with connective tissue disease. Jpn J Radiol 2010; 28 (6): 405-13.
15. Ueda N, Inoue Y, Himeji D, et al. Wegener's granulomatosis detected initially by integrated 18F-fluorodeoxyglucose positron emission tomography/computed tomography. Mod Rheumatol 2010; 20 (2): 205-9.
16. Beggs AD, Hain SF. F-18 FDG-positron emission tomographic scanning and Wegener's granulomatosis. Clin Nucl Med 2002; 27 (10): 705-6.
17. Soussan M, Abad S, Mekinian A, Dhote R, Eder V. Detection of asymptomatic aortic involvement in ANCA-associated vasculitis using FDG PET/CT. Clin Exp Rheumatol 2013; 31 (1 Suppl 75): S56-8.
18. Ito K, Minamimoto R, Yamashita H, et al. Evaluation of Wegener's granulomatosis using 18F-fluorodeoxyglucose positron emission tomography/computed tomography. Ann Nucl Med 2013; 27 (3): 209-16.
19. Soussan M, Abisror N, Abad S, et al. FDG-PET/CT in patients with ANCA-associated vasculitis: case-series and literature review. Autoimmun Rev 2014; 13 (2): 125-31.
20. Bertagna F, Treglia G, Rossini P, Giubbini R. An unusual orbital localization of wegener granulomatosis detected by 18F-FDG PET/CT. Clin Nucl Med 2014; 39 (8): 711-2.
21. Ito K, Minamimoto R, Yamashita H, et al. 18F-FDG PET/CT findings preceded elevation of serum proteinase 3 antineutrophil cytoplasmic antibodies in Wegener granulomatosis. Clin Nucl Med 2014; 39 (1): e67-8.
22. Chirinos JA, Tamariz LJ, Lopes G, et al. Large vessel involvement in ANCA-associated vasculitides: report of a case and review of the literature. Clin Rheumatol 2004; 23 (2): 152-9.
23. Braun JJ, Kessler R, Constantinesco A, Imperiale A. 18F-FDG PET/CT in sarcoidosis management: review and report of 20 cases. Eur J Nucl Med Mol Imaging 2008; 35 (8): 1537-43.
24. Basu S, Saboury B, Werner T, Alavi A. Clinical utility of FDG-PET and PET/CT in non-malignant thoracic disorders. Mol Imaging Biol 2011; 13 (6): 1051-60.
25. Jain V, Hasselquist S, Delaney MD. PET scanning in sarcoidosis. Ann N Y Acad Sci 2011; 1228: 46-58.